Additively Manufactured "Smart" RF/mm-Wave Packaging Structures

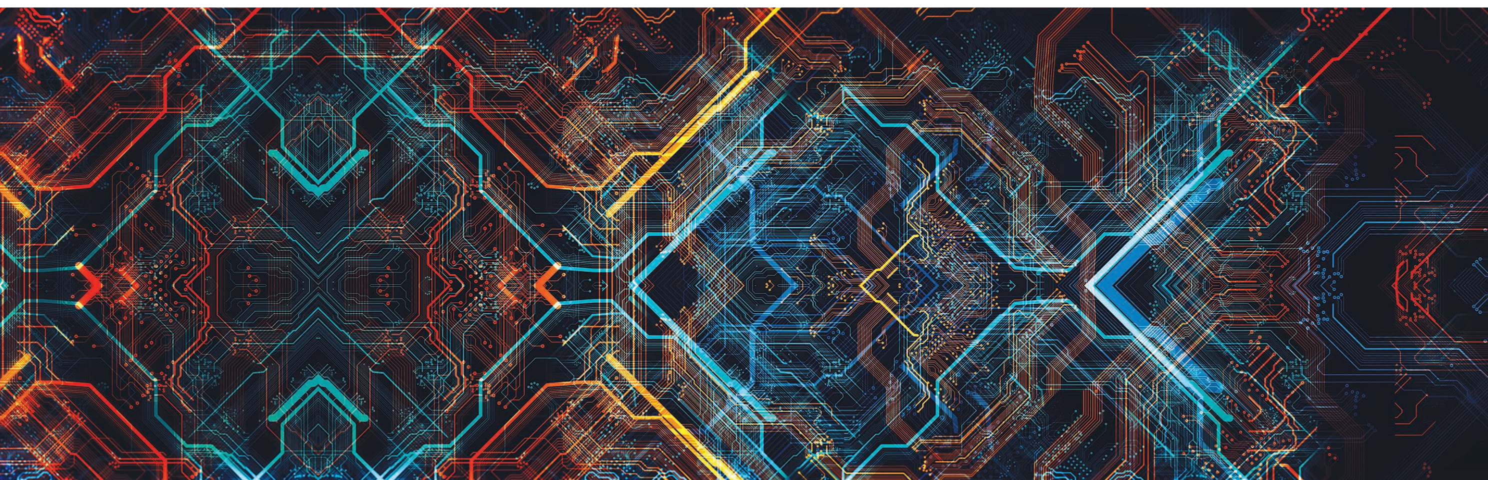

Xuanke He, Kexin Hu, Yepu Cui, Ryan Bahr, Bijan Tehrani, and Manos M. Tentzeris

5G and Internet of Things (IoT) technologies are rapidly expanding fields, utilizing cutting edge processes and manufacturing techniques that enable wide connectivity coverage and promise to connect billions of devices in all different types of environments. This critical requirement of ubiquitous implementation necessitates an adaptive system that can be easily modified on demand to be utilized in different areas of deployment.

Xuanke He (xhe53@gatech.edu), Kexin Hu (khu63@gatech.edu), Yepu Cui (yepu.cui@gatech.edu), Ryan Bahr (ryanbahr@gmail.com), Bijan Tehrani (bijanktehrani@gmail.com), and Manos M. Tentzeris (etentze@ece.gatech.edu) are with the School of Electrical and Computer Engineering, Georgia Institute of Technology, Atlanta, Georgia, 30332-0250, USA.

Digital Object Identifier 10.1109/MMM.2022.3173479
Date of current version: 8 July 2022

Authorized licensed use limited to: Georgia Institute of Technology. Downloaded on August 17,2022 at 17:26:24 UTC from IEEE Xplore. Restrictions apply.

This is where additive manufacturing (AM) can play a critical role. AM is a digital technology where information about the object's structure is stored digitally and fabricated using a device, such as a printer, that can recreate the structure in the real world. AM is a technology that can quickly iterate through designs for rapid prototyping, and its low cost of operation means that AM is a is a revolutionary tool for massively on-demand customization of electronic designs. In addition, AM enables novel, previously unrealizable integration techniques, which allows users to build their custom designs and package electronics in a way that is both space saving and low loss while setting the foundation for realization of massively "tile-by-tile," scalable multiple-input/multiple-output (MIMO) systems and reconfigurable intelligent surfaces.

This article focuses on utilizing a combination of various AM techniques to achieve innovative, customized RF packaging designs. It begins with a discussion of the benefits of AM technologies and its applications to packaging, with a comparison of various AM technologies including their pros and cons in printability, integration capability cost, and mechanical/physical reliability. It then presents a variety of these novel "smart" packaging solutions by combining two of the most commonly used AM technologies, 3D printing, and inkjet printing. These tools allow for rapid iterations just by changing the design file. The combination of inkjet and 3D printing has led to the first fully printed millimeter-wave (mm-wave) MCM (Figures 1 and 2) and system-on-antenna (SoA) modules (Figure 3), the first (fully printable) "ramp" interconnects (Figures 4 and 5), and the first fully printable "morphing"/"self-monitoring" packages (Figure 6)—all of which are covered in detail in this article. Specifically, the article will focus on four main topics regarding AM packages. First, a novel system-integration design, which leverages 3D printing's antenna-fabrication capability and the versatility of inkjet printing to print metals on abnormal surfaces to create a SoA. This system combines the additive benefits of both inkjet and 3D printing to embed electronics directly into the antenna surface. Second, a 3D-printed flexible package with an on-package antenna is demonstrated, featuring heterogenous integration along with integrated circuits (ICs) and energy-harvester embedding. Third, additively manufactured encapsulants are explored, which enable integrated "smart" packaging features not realized in traditional epoxy molding. Finally, inkjet and, more recently, aerosol jet printing are used to evaluate, all-additive packaging techniques that replace traditional wire/ribbon bond interconnects with AM "ramp" topologies. A schematic demonstrating a fully 3D-integrated module is shown in Figure 7. This system supports a compact integration of different components into one module by incorporating AM. The core substrate can be 3D printed with cavities of customized shapes and dimensions for embedding ICs; meanwhile, the microfluidic channel for heat dissipation can be directly formed during printing. Antenna in package (AiP) and smart encapsulation can be inkjet printed onto the top layer, then electromagnetic interference (EMI)-shielding structures can be 3D printed in compatible module materials/surfaces with the frequency-selective pattern directly inkjet printed. By combining various AM technologies, 3D-integrated designs with unprecedented complex structures and functionalities can be achieved for 5G/IoT modules up to at least mm-wave/subterahertz (THz) frequency ranges.

©SHUTTERSTOCK.COM/SPAINTER_VFX

AM for Packaging

The electronics industry has always strived to create higher performance, higher density, and smaller chips due to Moore's law. To pack even more chips into denser devices, packaging is increasingly being exploited to realize high-performance electronics in today's age. With 5G technologies, high-frequency mm-wave RF devices need to also be packaged in high-performance and high-density packages, along with logic ICs and passive components. AM has demonstrated the potential to introduce new packaging techniques that are difficult or even impossible to implement using traditional technologies, offering solutions to integration in mm-wave RF frequencies.

AM can be divided into several categories. Two prominent additive methods in printing circuit structures include aerosol jet and inkjet printing. These are 2.5D technologies that enable multilayer and multimaterial printing capability. Although these methodologies can deposit material in the x- and y-planar directions, the z direction (vertical height), that is, the height that can be printed, features only single or low double-digit-micron thicknesses. For true 3D structures, 3D printing technologies such as fused deposition modeling (FDM), stereolithography (SLA), and selective laser sintering (SLS) are utilized to push the vertical dimension up to hundreds of microns or even tens of millimeters. FDM is the most common type of 3D printing, with a wide range of applications [1] that uses heated extrusion to deposit thermoplastics and build up the structure layer by layer, while SLA achieves this using a photopolymer resin. SLS uses a high-power laser to fuse the small particles of powder materials. The capabilities and limitations of these technologies are listed in Table 1.

Authorized licensed use limited to: Georgia Institute of Technology. Downloaded on August 17,2022 at 17:26:24 UTC from IEEE Xplore. Restrictions apply.

AM material deposition is a relatively new technology compared to more mature processes like low-temperature cofired ceramics. Ceramic technology is widely used in high-frequency applications due to its excellent thermal properties and low-RF losses [2]. Typical dielectrics (HD100) in these processes have a very low tanδ of 0.003 [3] and are well characterized up to 110 GHz [4]. However, these processes utilize subtractive-masking techniques, which increases the cost of fabricating customized devices. AM's advantage is that there is no additional cost to retool, making it a perfect choice for prototyping, and low-to-medium production runs.

Multichip Module and SoA Electronics Integration

Effective packaging and integration are critical to creating complex electronic modules from individual components. With respect to RF components for 5G and IoT, the packaging of RF electronics must also take into consideration antenna integration for transmitting and receiving wireless signals. The introduction of AM, with 3D and inkjet printing, allows highly customizable packages and integration techniques [15]. One of these novel methods is the integration of RFICs onto the antenna surface/volume, called *SoA*.

SoA leverages the flexibility of AM, primarily 3D and inkjet printing. This fabrication process uses AM to embed monolithic microwave IC (MMIC)-active devices, feeding lines, and heat-management components onto custom 3D-printed antennas [16]. By combining the ideas behind system-on-chip (SoC)/system-on-package (SoP)/AiP and 3D-printed antennas, the SoA concept was created to incorporate the benefits of high integration seen in SoC/SoP/AiP and on-chip/package antennas in a low-cost fashion, while being easily realized using customizable AM techniques. The preliminary demonstrations of additively manufactured planar-phased arrays including cavity embedded packaged ICs are reported in [17]. In this work, a phase shifter was integrated along with a patch antenna element, proving the first steps in fabricating fully functional, wideband phased-array antenna elements at the X band. Gjokaj et al. [18] reported a compact receiver module in a

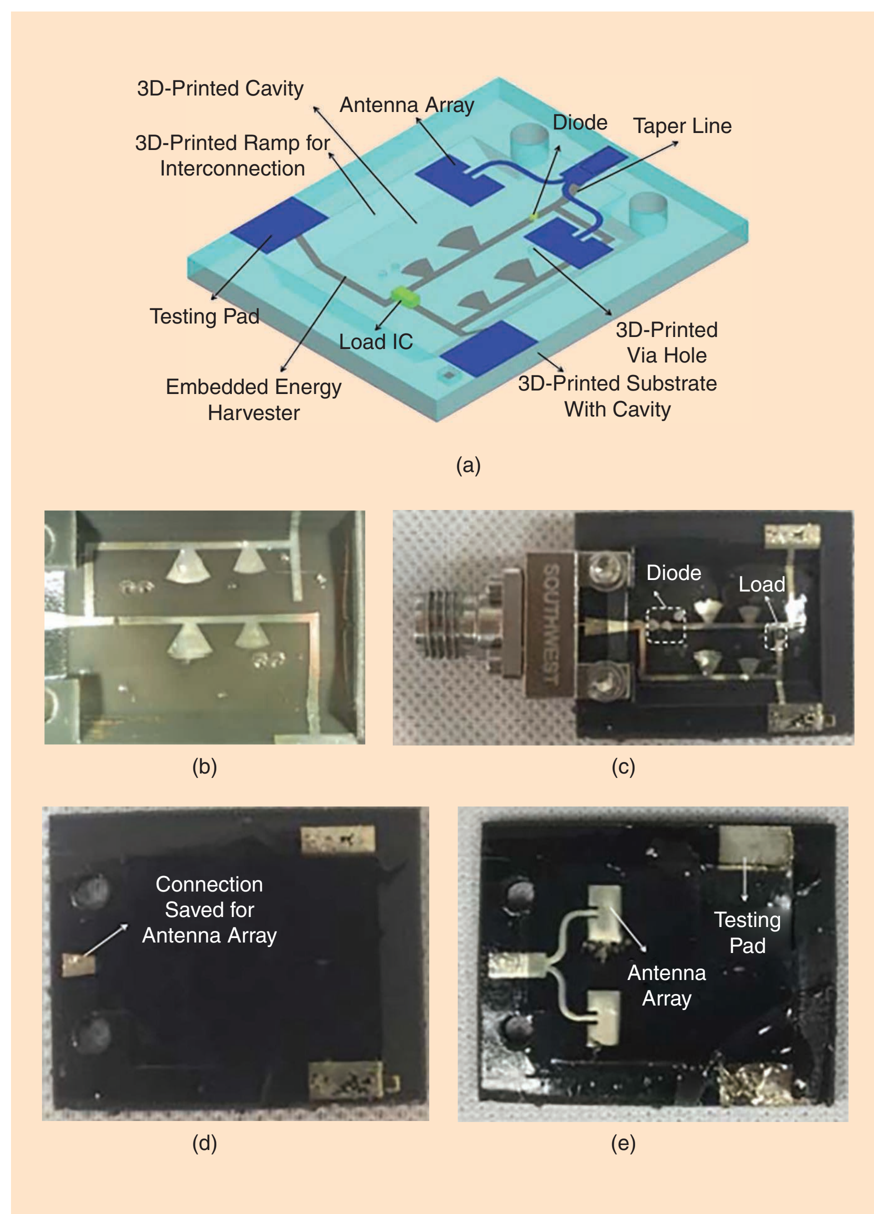

Figure 1. *(a) A flexible, additively manufactured packaged RF module, shown in layer-by-layer detail, beginning with (b) an encapsulated inkjet-printed support circuitry layout with radial stubs within a 3D-printed trapezoidal cavity featuring inkjet-printed ramp interconnects, (c) integration of a rectifying diode and proof-of-concept evaluation load IC, (d) a cavity-filling encapsulation layer of the IC and the supporting circuitry and (e) an SoP antenna array used at 26-GHz energy harvesting [22].*

Authorized licensed use limited to: Georgia Institute of Technology. Downloaded on August 17,2022 at 17:26:24 UTC from IEEE Xplore. Restrictions apply.

3D-printed Vivaldi antenna, however, this work still uses traditional printed circuit board (PCB) technology to interface with a 3D-printed antenna and is therefore not fully additively manufactured.

By embedding chips within antenna structures, entire systems can be fabricated directly attached to the antenna, eliminating the need for flanges and coax transitions and cables, which drastically reduce system size and loss. The additional size is minimized by eliminating the need for a PCB because the electronic circuits are built directly on the antenna. This can be achieved only with AM techniques as the traditional chip-/PCB-fabrication methods are not suitable for structures such as horn antennas due to their inherent structural nonuniformities. The SoA makes use of valuable space on the antenna, which traditionally would not have been utilized in the SoA work reported in [16]. Without loss of generality, the proof-of-concept application in this work is a radar transmitter device that can be used for tracking applications. This requires a variable-frequency source with frequency control. A Ku-band amplifier and voltage-controlled oscillator (VCO) are embedded into a 3D-printed horn antenna with customized cavities and connected and selectively metallized using inkjet-printed gap-filling interconnects to enable transmission of Ku-band signals for radar. The fully AM of the SoA module consists of four critical steps: 1) 3D printing and metallizing the antenna structure with the built-in cavity IC housing; 2) selectively metallizing the microstrip antenna feed; 3) attaching chips and inkjet printing the gap-filling material and RF and dc interconnects between VCO, amplifier, and antenna feed; and 4) 3D printing the heatsink structure for heat dissipation.

The antenna chosen for this application is a sectorial horn antenna that is 3D printed using Formlabs' Form 2 printer, utilizing the -temperature material

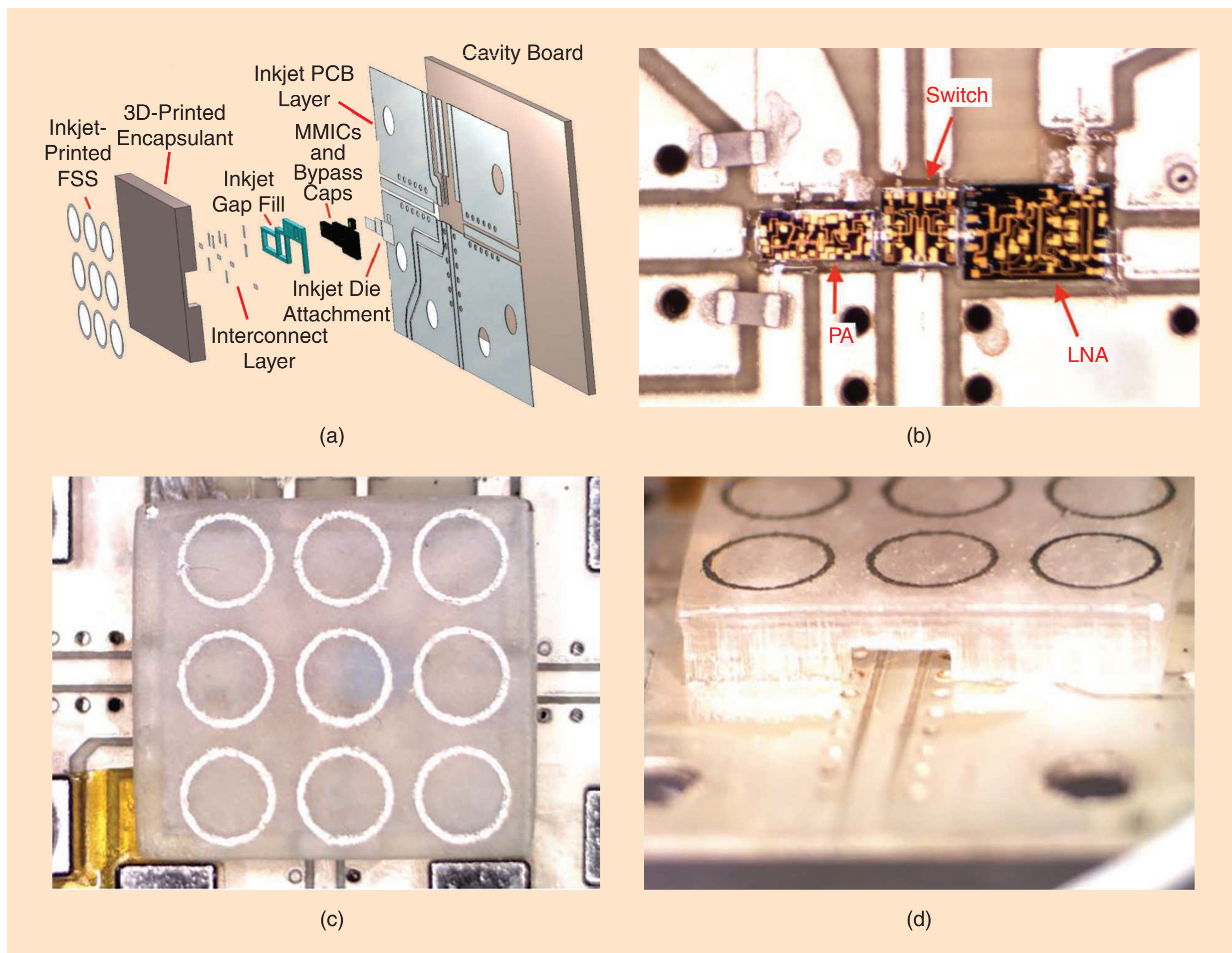

Figure 2. *(a) An exploded view of the complete encapsulated RF front-end MCM with an additively manufactured multilayer structure. (b) A nonencapsulated mm-wavefront-end MCM fabricated using inkjet printing (c) A 24-GHz FSS inkjet printed on top of the 3D-printed encapsulation. (d) A perspective image showing the cavity and the FSS-enabled "smart" encapsulation of the front-end MCM [15]. LNA: low-noise amplifier; PA: power amplifier.*

Authorized licensed use limited to: Georgia Institute of Technology. Downloaded on August 17,2022 at 17:26:24 UTC from IEEE Xplore. Restrictions apply.

with a standard WR42 waveguide feed section. A specialized high-temperature resin was used because of its heat-deflection temperature of 239 °C, which means that the structure of the antenna will not bend due to later sintering steps. Cavities are built into the walls of the antenna, which houses MMICs and the microstrip feed. The cavities are designed to be flat and in line with the surface of the antenna, which minimizes the losses associated with packaging of the ICs. A seed copper conductor layer with 3-µm thickness is electroless deposited onto the structure and grown by electroplating to approximately 7.9-µm, allowing for high conductivity. The completed SoA is presented in Figure 3 and the measured results are shown in Figure 3(d), where the tuning voltage is changed, resulting in a frequency-shifted amplified signal. The frequency shift down from Ku-Band frequencies is due to an attached mixer on the spectrum analyzer. The total system loss due to packaging was de-embedded and calculated to be 2.5–2.8 dB.

This SoA design demonstrates the versatility of AM. The electronic circuitry is built onto an irregular surface, which also doubles as the transmitter device. The implication of this research enables designers to utilize nonplanar surfaces as integration layers for RF electronics. This allows antennas to be placed anywhere, conformally onto irregular surfaces as needed, and the customized nature and rapid manufacturing capability of AM facilitates this. Future work regarding SoA includes further leveraging the benefits of AM by utilizing ad hoc components, where users can add or remove small subsystems to build larger systems for phased-array and other wireless applications.

TABLE 1. The advantages and disadvantages of various AM printing technologies.

Printing Technology	Advantages	Disadvantages
Aerosol jet printing	• High print resolution (<10 μm) [5] • Wide range of printable materials with various viscosities of ink viscosity • Conformal printing on curved surfaces • Nozzles using sheath gas protect nozzles from damage/clogging, leading to reliable and repeatable printing.	• High print resolution leads to slow print time • Difficult to bring to manufacturing scalability due to nozzle cost • Higher operating cost due to additional necessary units to create droplet mist and focused carrier gas stream [6].
Inkjet printing	• Mature technology, wide range of manufacturers, leading to low cost and high nozzle count for quick printing compared to aerosol • Low-cost nozzles and adjustable printing densities for thin- and thick-film deposition • Roll-to-roll production capability for rapid, high-volume manufacturing [7].	• Materials/inks are limited by their physical properties such as viscosity, surface tension • Limited nozzle lifetime due to clogging after periods of nonuse • Nozzle-cleaning procedures (purging, spitting) waste ink • Generally lower resolution than aerosol; however, low-volume production/prototype systems have achieved submicron resolutions [8].
FDM	• Low cost and widely available • Wide range of available filaments for a variety of properties and applications, such as flexible, conductive, or thermal, can be synthesized [9] • Easy to swap to different extruders for multimaterial printing [10].	• High surface roughness requires postprocessing, making it unsuitable for high-frequency mm-wave applications [11] • Low resolution mainly limited by nozzle's extruder dimensions; typical nozzle is generally on the order of hundreds of microns, meaning that the minimum feature size must be higher than the nozzle diameter [12] • Low thermal tolerances based on the nature of thermoplastics.
SLA	• High resolution, limited by the laser spot size [13], widely available, and low cost • Low surface roughness on the order of 100 s of nanometers, making surfaces excellent for printing conductive traces [14] • Digital light processing- or liquid crystal display-based SLA exposes patterns in a single exposure, allowing for quick fabrication.	• Materials must be ultraviolet or light curable or able to be suspended in photopolymer resins, limiting the types of materials used • Cleaning and postcuring of SLA-printed materials takes time.
SLS	• Lower material cost due to reusable powder materials • No support structure is required, thus suitable for complex design • Fast production rate due to a high-power laser.	• Materials must be powder based to be fused by a high-power laser, limiting the choices of materials • Higher surface roughness because of the use of powder materials.

Authorized licensed use limited to: Georgia Institute of Technology. Downloaded on August 17,2022 at 17:26:24 UTC from IEEE Xplore. Restrictions apply.

Flexible "Morphing"/"Self-Monitoring" So/iP Using AM

Extending functionality in AM packaging beyond the integration of passive structures is the next big step of AM, especially as heterogeneous AM with multiple materials—particularly for RF/mm-wave electronics—continues to be improved upon. These rapidly developing tools enable new combinations of materials, structures, and topologies. Of these materials, flexible electronics has seen significant growth to facilitate wearable electronics more conformal to human biology as well as to support various health applications.

Various flexible materials have been characterized for flexible 3D printing, including FDM materials such as thermoplastic polyurethane elastomer and Formlabs' flexible SLA resin [19], [20]. Flexible 3D structures can be more challenging to fabricate as relatively thick 3D topologies underlying material layers act as support structures for subsequent layers (see Figure 1). Under the stresses of many subsequent 3D printing processes, these layers can buckle/deform/flex while causing inaccurate solidification of thermoplastics and resins. With the integration of both flexible 3D printing and inkjet deposition of silver inks, 3D-flexible electronics of practically any shape can be realized.

Taking advantage of this flexibility derived by the combination of two AM techniques, it is possible to create heterogeneous packages that can utilize nonplanar interconnects across ICs of various heights, with

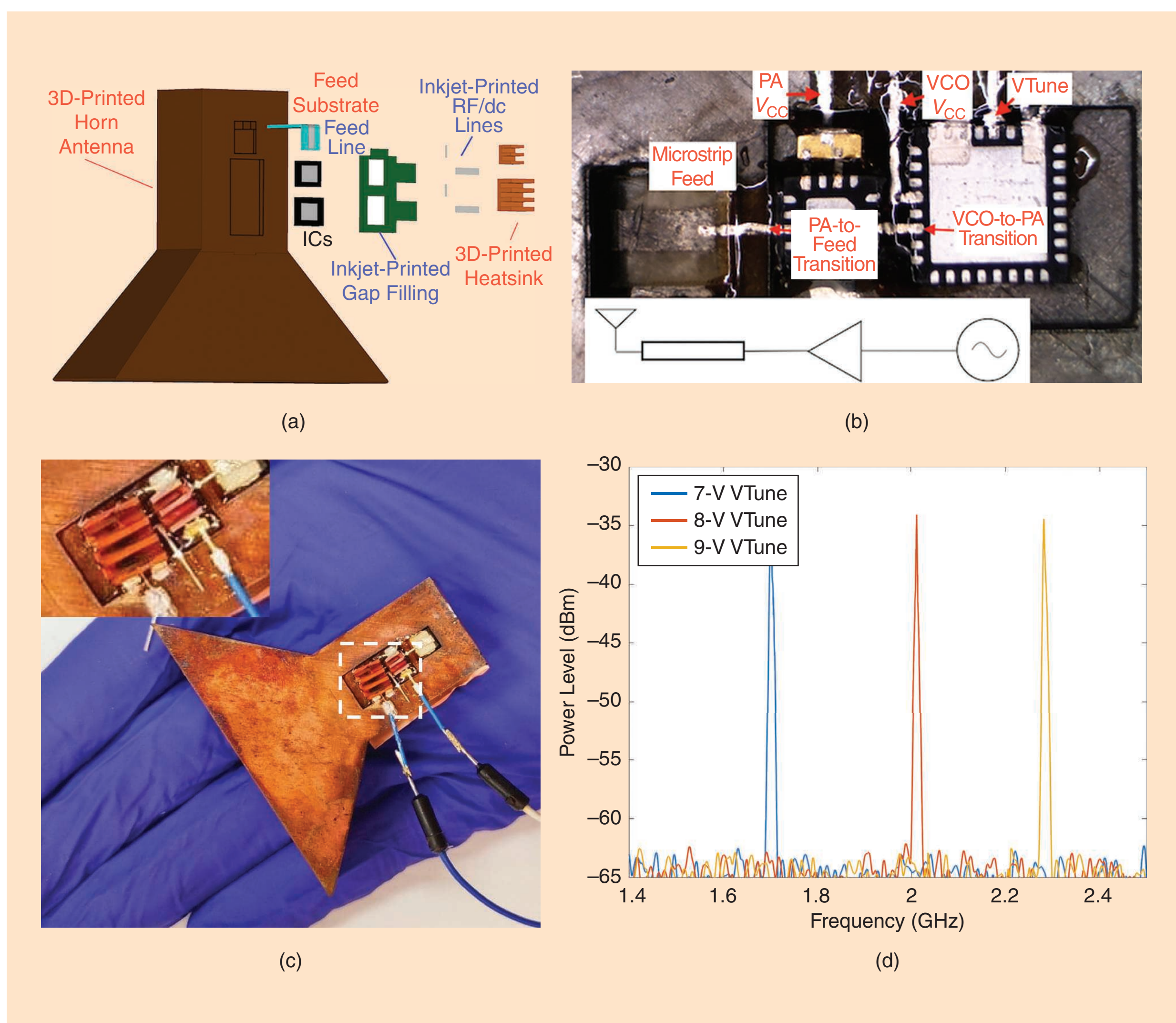

Figure 3. *(a) An exploded view of the SoA proof-of-concept topology. With the exception of the ICs, all other components were fully additively manufactured. (b) A fully printed SoA with RF and dc inkjet-printed lines and the equivalent schematic. (c) The top view of the SoA module prototype with an enlarged heatsink (inset). A heatsink is required because the chip generates a considerable amount of heat. (d) The received power level from the SoA, with different tuning voltages demonstrating practical systems applicability [16]. PA: power amplifier.*

Authorized licensed use limited to: Georgia Institute of Technology. Downloaded on August 17,2022 at 17:26:24 UTC from IEEE Xplore. Restrictions apply.

nonplanar ramps enabling improved performance, as discussed in the previous section. Utilizing a custom-built stereo-lithography machine that enables ex situ midprint processing before printing continues, the integration of active ICs is demonstrated in a flexible package [21]. In this case, an on-package antenna is demonstrated in the mm-waveband of 24.4 to 30.1 GHz, with chip integration demonstrated for flexible antennas on package (AoP) to achieve flexible modules.

With this heterogeneous approach, many topologies can be realized through the integration of processes that traditionally do not coexist. The integration of full systems in flexible packages enable compact electronic devices that may possibly get implanted—the next stage of wearables—where devices are integrated directly into the human body. For implants to be successful, the modules need to consume extremely minuscule amounts of power off harvested ambient energy and backscattering principles. An AoP design with flexible substrates and ICs is demonstrated in [22], with additional integration of an mm-wave/5G energy harvester, enabling energy to be harvested beyond 0.2 m with enough energy to power a timer circuit [22]. When considering effective isotropic radiated power (EIRP) limitations for 5G communications, the range can be extended beyond 1 m. With the use of energy harvesting, modules can become perpetually autonomous, enabling extended life while powering more complex electronics for additional information, which may be used from biological monitoring, low-power wearables, and other IoT applications. Using flexible substrates and 3D-printed structures, AoP designs can be transformed into shape-changing “morphing” RF designs with unprecedented capabilities of mechanical tunability as well as integrability within conformal/compressible platforms [see Figure 6(a)]. Using integrated inkjet-printed 2D strain sensors and machine learning algorithms, the impact of the mechanical bending in the performance of the

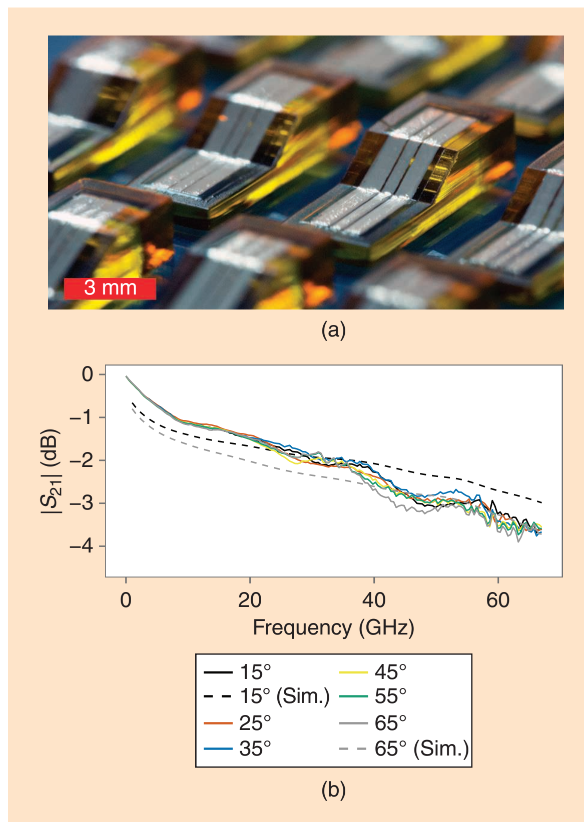

Figure 4. *(a) A 3D-inkjet-printed sloped “ramp” TMV with inkjet-printed coplanar waveguide interconnects (35° slope). (b) $|S_{21}|$ measurements and simulations of printed TMVs with varying slopes [25]. Sim.: simulated.*

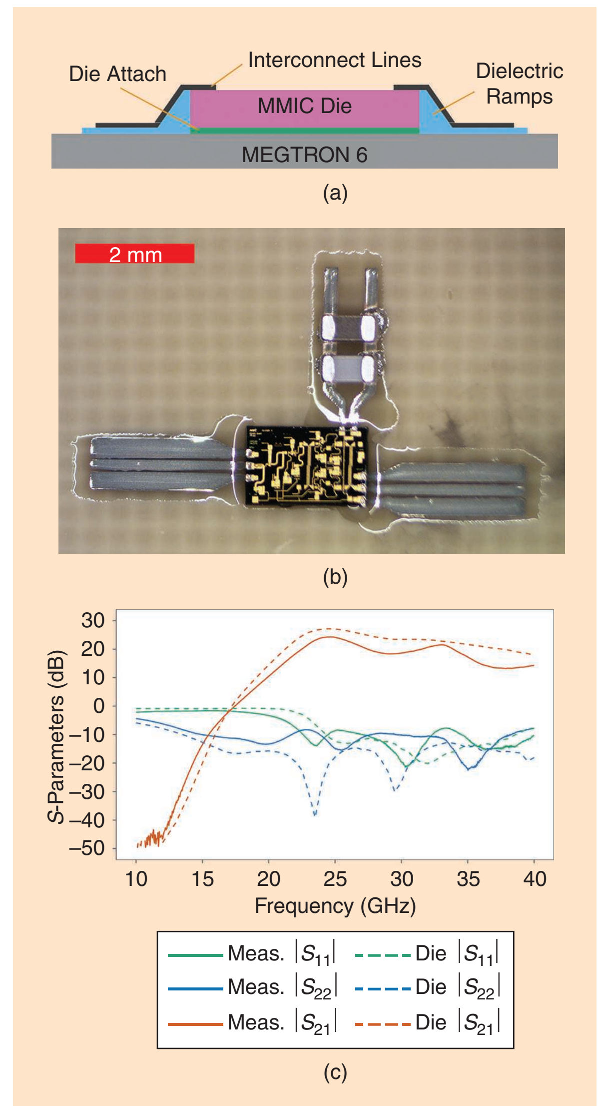

Figure 5. *(a) The 2D cross section of a ramped interconnect structure. (b) A full-device view of the packaged MMIC with RF and dc interconnects. (c) Measured S-parameters for the inkjet-printed ramp interconnects with a Ka-band LNA MMIC [33]. Meas.: measured.*

Authorized licensed use limited to: Georgia Institute of Technology. Downloaded on August 17,2022 at 17:26:24 UTC from IEEE Xplore. Restrictions apply.

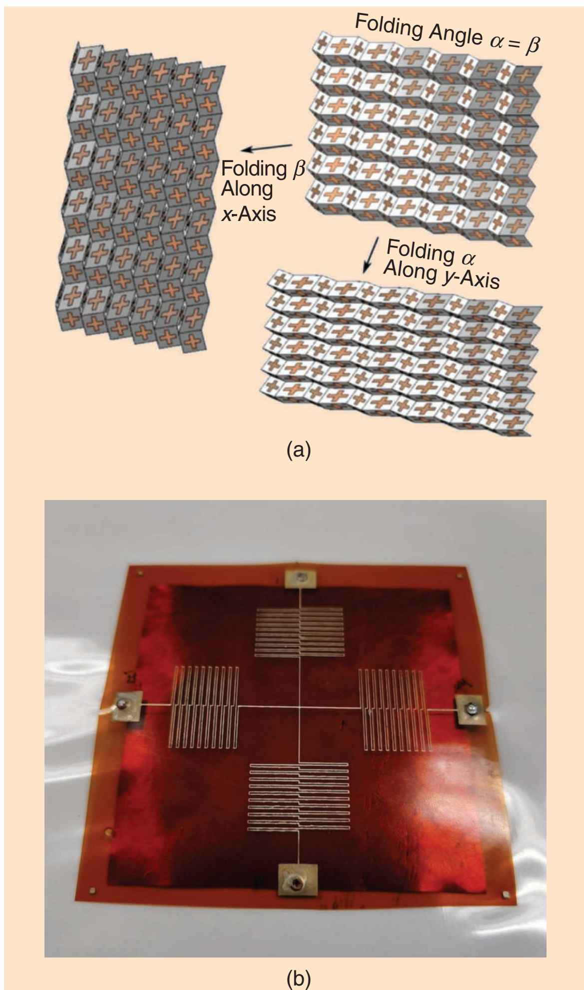

Figure 6. *(a) An origami-inspired, "eggbox" shape-changing "morphing" flexible RF packaging structure [23] and (b) inkjet-printed, 2D strain ("bending deformation") sensor for flex compensation in flexible RF packages/modules [24].*

"morphing" RF package/module can be accurately predicted ("self-monitoring" packages) and calibrated out, effectively reverting to "zero-deformation" optimal RF performance [Figure 6(b)].

Printed "Smart" Encapsulants for mm-Wave Systems

Across the field of microelectronic packaging, industry standards for IC encapsulation rely on the process of epoxy molding, a process based on thermal transfer molding of epoxy compounds for the protective sealing of IC dies. Standard epoxy molding processes offer minimal freedom for SiP integration, where the tooling and upscale required for diverse encapsulant functionality is unfeasible in practical production-level settings. This section outlines the design principles and fully additive processes involved with the development of "smart" microelectronic encapsulants for wireless systems. The combination of inkjet and 3D printing technologies is used to realize encapsulants with integrated functionality, including microfluidic channels for thermal management, package-integrated lenses, and through-mold-via (TMV) interconnects for wireless SiP modules.

Specifically, the use of SLA 3D printing with two general resin varieties is highlighted, including a standard acrylate-based resin (Vorex) and ceramic-loaded resin (Porcelite). The accurate dielectric characterization of these SLA materials is necessary to ensure accurate simulations and designs. WR-12 waveguide fills with 3.01 mm × 1.55 mm × 1-mm dimensions need to be fabricated to fill 1-mm-thick WR-12 spacer shims. The E-band S-parameters are measured, followed by implementation of iterative models, satisfying Kramers–Kronig relations to extract the ε_r tan δ of the

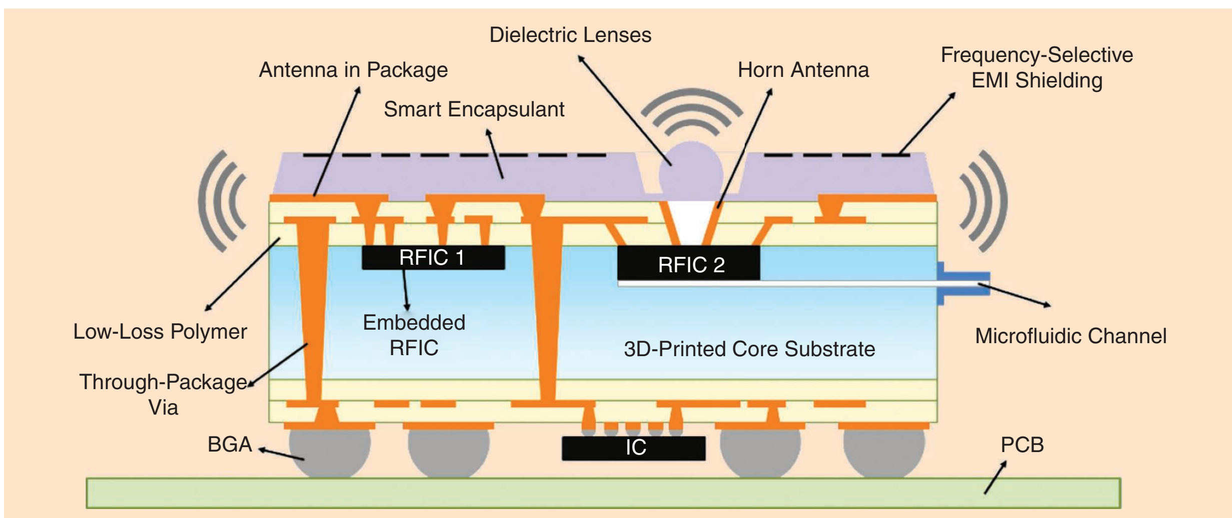

Figure 7. *An overview demonstrating 3D-integration techniques enabled using AM for 5G/IoT module systems. BGA: ball grid array; PCB: printed circuit board.*

Authorized licensed use limited to: Georgia Institute of Technology. Downloaded on August 17,2022 at 17:26:24 UTC from IEEE Xplore. Restrictions apply.

printed materials, yielding an ε_r of 2.62 and 3.43 for the Vorex and Porcelite resins, respectively. As expected, the ceramic-loaded Porcelite material exhibits a higher ε_r due to the presence of high-ε_r ceramic composites. Tan δ measurements up to 95 GHz yield maximums of 0.019 and 0.026 for the Vorex and Porcelite samples, respectively, demonstrating their suitability for RF applications [25]. For applications that require low loss tangent, Rogers and Fortify released two materials with tan δ down to 0.0039 [26] at 10 GHz, and 3M also demonstrated an industry-first, 3D-printed polytetrafluoroethylene [27].

Arbitrarily Shaped SiP IC Encapsulants

The printing of an IC die encapsulant using the proposed SLA materials was demonstrated with the goal of replacing standard epoxy molding and stamping methods of package encapsulation [29]. In addition to being an ambient-pressure room-temperature fabrication process, SLA printing allows for the simple realization of selectively patterned and nontraditionally shaped encapsulation solutions while simultaneously maintaining tan δ within the same range of standard epoxy-molding compound materials [30]. Silicon dies with 280-μm thickness and areas of 2 mm × 2 mm and 3 mm × 3 mm were attached to a metallic quad flat no-lead package (QFN) lead frame using an inkjet-printed polymer-based ink. After the dies were attached, 5.5 mm × 5.5 mm × 1-mm encapsulations were printed directly onto the dies using the Vorex and Porcelite materials and the outlined processing conditions. This is accomplished by affixing the QFN lead frames to the build plate of the SLA printer to directly pattern the die encapsulations onto the lead frames. Figure 8 presents images of the printed Vorex and Porcelite encapsulations. In addition to the standard encapsulation, an SLA printing tool can be configured to fabricate nontraditional encapsulation shapes; for example, the dielectric lenses for package-integrated antennas depicted in Figure 8(e), on-package frequency-selective surfaces (FSSs) for filtering and EMI mitigation presented in Figure 8(f), and package-integrated microfluidic networks for thermal management displayed in Figure 8(g). These novel package shapes can be achieved by simply changing the 3D model in the SLA printing tool, highlighting the on-demand reconfigurable nature of this technology for diverse application-specific packaging applications.

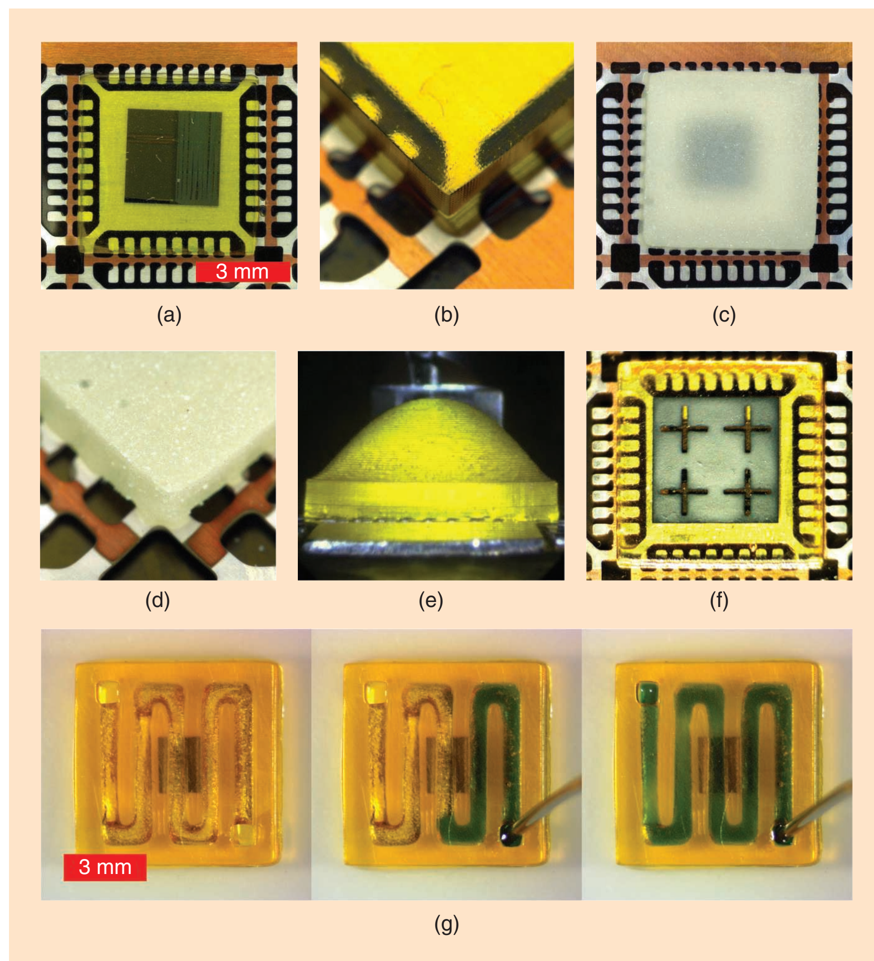

Figure 8. *3D-printed die encapsulants on a metallic QFN leadframe. A Vorex encapsulation with (a) a top view and (b) perspective view, and a Porcelite encapsulation with (c) a top view and (d) perspective view. A Vorex encapsulant with (e) a dielectric lens, (f) an FSS integration [14], and (g) a microfluidic network [28].*

Fully Printed Sloped ("Ramp") TMVs

SLA 3D printing technology can be combined with existing inkjet printing technology to realize the postprocess fabrication of on-package components, including passive components, antennas, sensors, and metamaterial structures [14], [25]. With the ability to inkjet print electronic structures directly onto a 3D-printed encapsulant, interest is placed onto how these structures can interface with a molded IC within the package. The concept of directly interconnecting a molded IC die to an external plane of its encapsulation is an area not

Authorized licensed use limited to: Georgia Institute of Technology. Downloaded on August 17,2022 at 17:26:24 UTC from IEEE Xplore. Restrictions apply.

widely covered in literature. Amkor Technology, Inc. (Chandler, Arizona, USA) demonstrated a TMV process for PoP integration, however, the interconnects were limited to solder balls typically used with ball grid array packages [31]. Therefore, the development of printed mm-wave TMVs is an essential task for the realization of 3D "smart" encapsulants for wireless device packages. Figure 9 outlines a conceptual process flow for the fabrication of arbitrary slope ("ramp"), TMVs, and SiP wireless encapsulants combining 3D and inkjet printing [28]. Fabrication begins with the inkjet printing of TMV interconnects directly onto the pads of the IC, leading up to the inkjet-printed sloped "ramp" conductive line onto the 3D-printed encapsulant wall and ending with the final printed interconnect section on the top plane of the encapsulant. Next, 3D printing is used to seal the partial encapsulant, leaving the inkjet-printed interconnects exposed at the new filled-cavity top plane of the encapsulant. Multilayer antenna array and/or passive components are then inkjet printed directly onto the encapsulant, interfacing with the TMVs leading up from the die. Finally, 3D printing is used to seal the wireless package.

This integration of inkjet printing with 3D printing technology requires an analysis of the capabilities of this typically 2D/2.5D technology in truly 3D applications. To evaluate SLA 3D printing technology integration with inkjet printing for mm-wave packaging, ramped interconnect structures with slopes ranging from 15–75° were characterized with the Vorex SLA material [25]. The sloped TMV test vehicle was fabricated using a combination of SLA printing to realize the 3D sloped transitions and inkjet printing to pattern surface smoothening films and coplanar waveguide transmission lines. Figure 4(a) shows a perspective micrograph of the test vehicle containing multiple samples of the SLA ramps with varying slope. Insertion loss of the printed TMV interconnects measuring 6.6 mm in length was measured up to 67 GHz and presented in Figure 4(b), along with simulations for the two extreme cases (15 and 65°). All the slopes ranging from 15–65° exhibit an insertion loss between 0.5–0.6 dB/mm at 60 GHz. Further optimization of the transitions can be investigated through the inclusion of fillet and chamfer techniques for the 3D-printed ramp structures. The presented inkjet-printed 3D ramp interconnects yield a four-times reduction in insertion loss compared to standard wire-bond interconnects at 60 GHz [32].

Additively Manufactured Multichip Module Integration With "Smart" Encapsulations

mm-wave packaging encapsulation usually involves expensive processes that create air cavities over packaged devices to minimize dielectric loading of the chip. 3D printing can achieve encapsulation in a low cost and straightforward manner. To implement more compact and miniaturized RF multichip modules, inkjet-printed, gap-filled interconnects can be used to build communication between chips and circuit boards and connect MMICs placed inside 3D cavities of arbitrary shapes to out-of-cavity components and conductors. This method provides a shorter loop length, lower parasitic loss, and a more rugged structure. A fully additively manufactured multichip module (MCM) with a "smart" FSS-enabled encapsulation is shown in Figure 2. Figure 10 illustrates the utilized gap-filling interconnects realized by inkjet printing. The proof-of-concept AM MCM module in Figure 2 incorporates the gap-filling interconnects by inkjet printing SU8 into small gaps of 400 μm in width and 100 μm in depth, representing the typical gap between a 3D-printed IC-embedding cavity wall with a height of 100 μm and an IC placed within the cavity, along with an inkjet-printed 75 µm wide interconnecting conductive line bridging two 50-Ω lines that could be located both on top of an additively manufactured substrate, such as a Megtron 6, or one on the substrate and the other on the IC inside the cavity. The measured insertion loss of this interconnect over 10–40 GHz is approximately

mm-wave packaging encapsulation usually involves expensive processes that create air cavities over packaged devices to minimize dielectric loading of the chip.

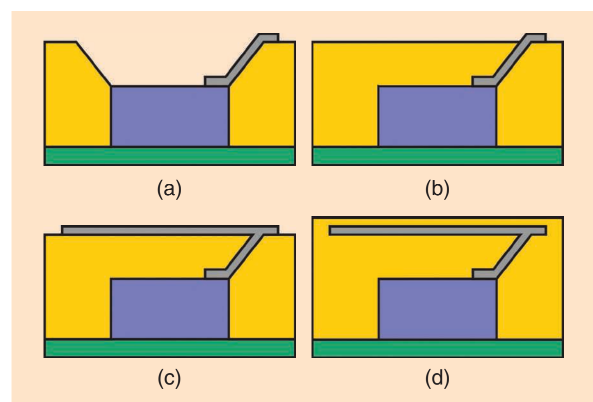

Figure 9. *A "smart" wireless-encapsulant process flow. (a) A 3D print-partial encapsulant (yellow) with die (purple) and inkjet print-sloped "ramp" TMV (gray). (b) A cap-partial encapsulant with photopolymer resin leaving an exposed TMV interconnecting to an embedded die. (c) An inkjet-printed antenna, passive, or other SiP component. (d) A 3D-printed final-sealing encapsulant [28].*

Authorized licensed use limited to: Georgia Institute of Technology. Downloaded on August 17,2022 at 17:26:24 UTC from IEEE Xplore. Restrictions apply.

0.5 dB. It has also been proved that this inkjet-printed, gap-filled interconnect features a better insertion loss/gain performance for low-noise amplifier (LNA) ICs compared with traditional transitions, such as ribbon bonds. The complete RF front-end MCM design is demonstrated in Figure 2(a), which includes a milled cavity board, an inkjet-printed PCB layer with RF MMICs connected by gap-filling interconnects, and a 3D-printed encapsulation with an inkjet-printed FSS. The only noninkjet-printed, front-end components are an ALH369 LNA as the receiver IC, TGA4036 as the transmitter IC, and TGS4302 as the switching module, as shown in Figure 2(b). The encapsulation is specifically designed and directly 3D printed on top of the front-end circuits. It is 1-mm higher than the circuits, and the encapsulant is 0.2-mm thick. An on-package 3 × 3 circular-ring FSS was then inkjet printed on top of this encapsulant for ambient shielding (EMI/EMC) purposes, as depicted in Figure 2(c). The targeted frequency range to be blocked lies in a 2-GHz band around 24 GHz. The measurements for this MCM with FSS capping shows an extra >18-dB isolation at 24 GHz and no effect on the $|S_{21}|$ performance compared to the same MCM without FSS capping. The advanced "smart" features and high customization in this design can be easily incorporated in 5G+/ mm-wave packages, thus enabling more complex functions such as EMI shielding [15].

AM "Ramp" Interconnects to Replace Bond Wires in mm-Wave RF Packages?

The traditional interconnects for MMIC gallium arsenide dies require ribbon or wire-bonding. These bonds are the interfaces that carry RF signals and need to be low loss and feature low parasitics and wideband. At mm-wave frequencies, bond wires can even generate radiation losses [34]. It is then necessary to optimize the shape and length of these interconnects to achieve desired performance targets for 5G and other high-frequency applications.

The novel "ramp" interconnect structures were first demonstrated in 2016 using inkjet printing technologies [35], and their use in practical MMIC topologies was further extended in [35], [36]. These interconnects form a smooth transition from substrate to a Ka-band LNA MMIC, with a loss of 0.57 dB/mm. The discrete MMIC-ramped packaging technique benefits from having a low loss interconnect with the MMIC placed directly onto the substrate without the need to machine cavities in the substrate, which is expensive and physically damaging to various, particularly flexible, substrates. The stack up of the ramped interconnects is shown in Figure 5(a), with the packaged MMIC presented in Figure 5(b), and S-parameters displayed in Figure 5(c). Lately, chaos-expansion-based numerical methods have allowed, for the first time, an accurate incorporation and modeling of practical AM tolerances and uncertainties in the optimization of RF/ mm-wave inkjet-printed ramp

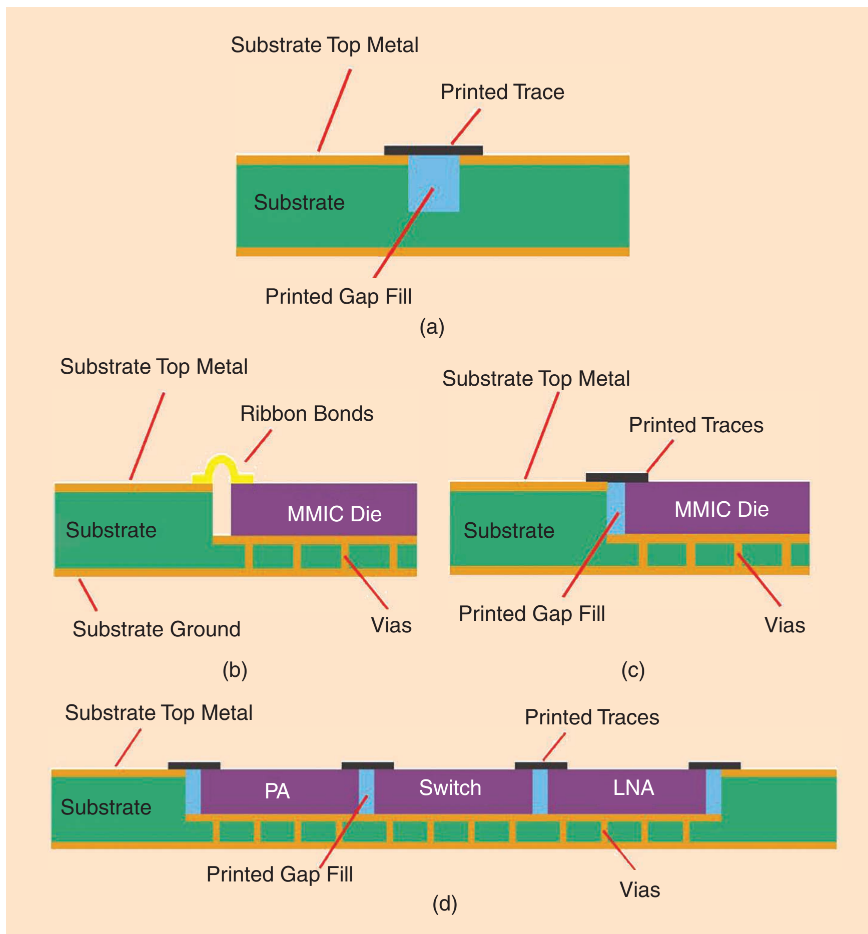

Figure 10. *A side-view schematics summary of the AM gap-filling interconnect topologies. (a) A printed trace interconnect over a printed gap fill to "emulate" a standard (continuous) microstrip transmission line. (b) and (c) A ribbon-bonded LNA MMIC interconnect comparison with an inkjet-printed LNA MMIC interconnect. (d) A fully inkjet-printed interconnected RF front-end MCM. PA: power amplifier.*

Authorized licensed use limited to: Georgia Institute of Technology. Downloaded on August 17,2022 at 17:26:24 UTC from IEEE Xplore. Restrictions apply.

interconnects in an approach that could be easily generalized to the optimization of additively manufactured integrated MCM modules up to sub-THz frequencies [29].

Recently, aerosol jet printing has also demonstrated "chip-first" packaging techniques where the packaging structure is built up around the chip [37]. Additionally with aerosol jet printing, due to its material printing flexibility, nanocomposite films composed of barium titanate are able to be deposited, which is used to fabricated capacitors for dc bypass. This is integrated alongside the package in a fashion similar to nanostructure (graphene, carbon nanotube)-based sensors that have been realized using inkjet printing [38], demonstrating a first for aerosol jet-printed packaging. The packaging loss for this aerosol jet technique is similar to that in [33] at 0.55 dB/mm at 15 GHz. The package is disclosed in Figure 11(a) and measured results of two printed packages are shown in Figure 11(b).

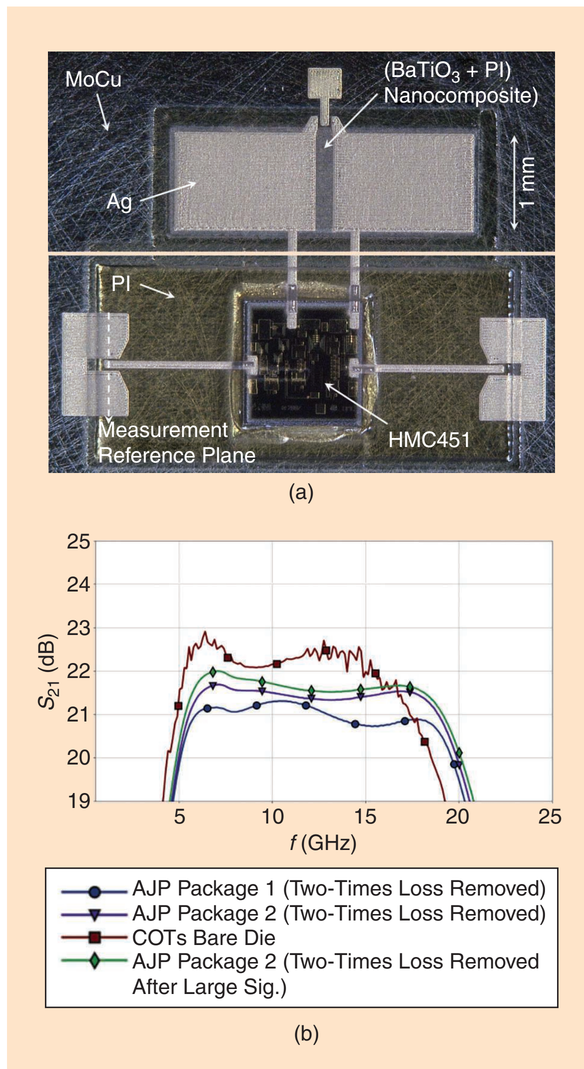

Figure 11. *(a) Aerosol jet-printed nanocomposite bypass capacitors. (b) A packaged MMIC using aerosol jet polyimide (PI) dielectric and silver nanoparticle interconnects. (c) Measured S-parameters for the aerosol jet-printed package with a bare die comparison [37]. MoCu: molybdenum copper; $BaTiO_3$: barium titanate; Ag: silver; COTS: commercial off-the-shelf; AJP: aerosol jet printing.*

Conclusions

In this article, numerous state-of-the-art AM packaging and integration approaches for RF electronics up to mm-wave frequency ranges were discussed, clearly highlighting unique capabilities of creating new and high-performance solutions for 5G and IoT devices. SoA features a novel system where the antenna structure is used to house the electronics, creating a "standalone" integrated system. The versatility of AM also facilitates the use of different antenna types for realization of SoA modules. Also, 3D-printed flexible packages featuring on-package antennas demonstrate the broad range of areas in which AM can be utilized for wireless electronics, including wearable and implantable applications. A novel packaging encapsulation method using AM is presented, enabling integrated "smart" features such as a dielectric lens, TMVs, and microfluidics into an otherwise overlooked part of IC packaging. This grants additional functionality to IC encapsulation. Finally, inkjet and aerosol printing were explored to create high performance, all additively manufactured packages, which exhibit low loss and demonstrate versatile capability integration using AM. All these AM techniques for RF/mm-wave packaging and integrated multichip modules are widely applicable to a variety of "rugged" wireless broadband 5G and IoT systems, potentially setting the foundation for large-scale smart city, smart wearable biomonitoring, smart agriculture, and autonomous car implementations as well as for massively scalable "tile-by-tile" MIMO systems and reconfigurable intelligent surfaces up to at least sub-THz frequencies.

Acknowledgments

The authors would like to thank the U.S. Air Force Office of Scientific Research Origami Center and National Science Foundation for supporting this work.

References

[1] K. H. Church *et al.*, "Multimaterial and multilayer direct digital manufacturing of 3-d structural microwave electronics," *Proc. IEEE*, vol. 105, no. 4, pp. 688–701, 2017, doi: 10.1109/JPROC.2017.2653178.

[2] K. K. Samanta, "Ceramics for the future: Advanced millimeter-wave multilayer multichip module integration and packaging," *IEEE Microw. Mag.*, vol. 19, no. 1, pp. 22–35, 2018, doi: 10.1109/MMM.2017.2759598.

[3] K. K. Samanta and I. D. Robertson, "Surfing the millimeter-wave: Multilayer photoimageable technology for high performance SOP components in systems at millimeter-wave and beyond," *IEEE Microw. Mag.*, vol. 17, no. 1, pp. 22–39, 2016, doi: 10.1109/MMM.2015.2487898.

Authorized licensed use limited to: Georgia Institute of Technology. Downloaded on August 17,2022 at 17:26:24 UTC from IEEE Xplore. Restrictions apply.

[4] K. K. Samanta, D. Stephens, and I. D. Robertson, "Ultrawideband characterisation of photoimageable thick film materials for microwave and millimeter-wave design," in *Proc. IEEE MTT-S Int. Microw. Symp. Dig.*, 2005, p. 4.

[5] "Aerosol jet® printed electronics overview," Optomec, Tech. Rep., Jan. 2014. [Online]. Available: URL:https://www.optomec.com/wp-content/uploads/2014/04/AJ_Printed_Electronics_Overview_whitepaper.pdf

[6] T. Seifert, E. Sowade, F. Roscher, M. Wiemer, T. Gessner, and R. R. Baumann, "Additive manufacturing technologies compared: Morphology of deposits of silver ink using inkjet and aerosol jet printing," *Ind. Eng. Chem. Res.*, vol. 54, no. 2, pp. 769–779, 2015, doi: 10.1021/ie503636c.

[7] R. R. Søndergaard, M. Hösel, and F. C. Krebs, "Roll-to-roll fabrication of large area functional organic materials," *J. Polym. Sci. B, Polym. Phys.*, vol. 51, no. 1, pp. 16–34, 2013, doi: 10.1002/polb.23192.

[8] *Super Inkjet Printer*. SIJTechnology, Inc., Tsukuba, Japan, 2020.

[9] A. C. de Leon, Q. Chen, N. B. Palaganas, J. O. Palaganas, J. Manapat, and R. C. Advincula, "High performance polymer nanocomposites for additive manufacturing applications," *Reactive Funct. Polymers*, vol. 103, pp. 141–155, Jun. 2016, doi: 10.1016/j.reactfunctpolym.2016.04.010.

[10] D. Espalin, J. Ramírez, F. Medina, and R. Wicker, "Multi-material, multi-technology FDM: Exploring build process variations," *Rapid Prototyping J.*, vol. 20, no. 3, pp. 236–244, Apr. 2014.

[11] B. Zhang, W. Chen, Y. Wu, K. Ding, and R. Li, "Review of 3d printed millimeter-wave and terahertz passive devices," *Int. J. Antennas Propag.*, vol. 2017, pp. 1–10, 2017.

[12] G. Franz. "What resolution can 3d printers print?" https://all3dp.com/3d-printer-resolution/

[13] H. Quan, T. Zhang, H. Xu, S. Luo, J. Nie, and X. Zhu, "Photo-curing 3d printing technique and its challenges," *Bioactive Mater.*, vol. 5, no. 1, pp. 110– 115, 2020, doi: 10.1016/j.bioactmat.2019.12.003.

[14] B. K. Tehrani, S. A. Nauroze, R. A. Bahr, and M. M. Tentzeris, "On-package mm-Wave FSS integration with 3d-printed encapsulation," in *Proc. IEEE Int. Symp. Antennas Propag. USNC/URSI Nat. Radio Sci. Meeting*, 2017, pp. 9–10.

[15] X. He, B. K. Tehrani, R. Bahr, W. Su, and M. M. Tentzeris, "Additively manufactured mm-Wave multichip modules with fully printed "smart" encapsulation structures," *IEEE Trans. Microw. Theory Techn.*, vol. 68, no. 7, pp. 2716–2724, 2020, doi: 10.1109/TMTT.2019.2956934.

[16] X. He, Y. Fang, R. A. Bahr, and M. M. Tentzeris, "Rf systems on antenna (SOA): A novel integration approach enabledby additive manufacturing," in *Proc. IEEE MTT-S Int. Microw. Symp. (IMS)*, Jun. 2020, pp. 1157–1160, doi: 10.1109/IMS30576.2020.9223793.

[17] M. Kacar *et al.*, "Phased array antenna element with embedded cavity and MMIC using direct digital manufacturing," in *Proc. IEEE Int. Symp. Antennas Propag. USNC-URSI Radio Sci. Meeting*, 2019, pp. 81–82, doi: 10.1109/APUSNCURSINRSM.2019.8888323.

[18] V. Gjokaj, J. Papapolymerou, J. D. Albrecht, B. Wright, and P. Chahal, "A compact receive module in 3-d printed vivaldi antenna," *IEEE Trans. Compon. Packag. Manuf. Technol.*, vol. 10, no. 2, pp. 343–346, 2020, doi: 10.1109/TCPMT.2019.2961345.

[19] R. Bahr *et al.*, "Rf characterization of 3d printed flexible materials – Ninjaflex filaments," in *Proc. Eur. Microw. Conf. (EuMC)*, Sep. 2015, pp. 742–745.

[20] T.-H. Lin, R. A. Bahr, and M. M. Tentzeris, *Additive Manufacturing AiP Designs and Applications*. Hoboken, NJ, USA: Wiley, 2020, ch. 9, pp. 267–291. [Online]. Available: https://onlinelibrary.wiley.com/doi/abs/10.1002/9781119556671.ch9

[21] T. Lin, R. Bahr, M. M. Tentzeris, P. M. Raj, V. Sundaram, and R. Tummala, "Novel 3d-/inkjet-printed flexible on-package antennas, packaging structures, and modules for broadband 5G applications," in *Proc. IEEE 68th Electron. Compon. Technol. Conf. (ECTC)*, 2018, pp. 214–220, doi: 10.1109/ECTC.2018.00041.

[22] T. Lin, S. N. Daskalakis, A. Georgiadis, and M. M. Tentzeris, "Achieving fully autonomous system-on-package designs: An embedded-on-package 5G energy harvester within 3d printed multilayer flexible packaging structures," in *Proc. IEEE MTT-S Int. Microw. Symp. (IMS)*, 2019, pp. 1375–1378, doi: 10.1109/MWSYM.2019.8700931.

[23] Y. Cui, R. Bahr, S. V. Rijs, and M. Tentzeris, "A novel 4-dof wide-range tunable frequency selective surface using an origami "egg-box" structure," *Int. J. Microw. Wireless Technol.*, vol. 13, no. 7, pp. 727–733, 2021, doi: 10.1017/S1759078721000799.

[24] X. He and M. M. Tentzeris, "In-package additively manufactured sensors for bend prediction and calibration of flexible phased arrays and flexible hybrid electronics," in *Proc. IEEE MTT-S Int. Microw. Symp. (IMS)*, 2021, pp. 327–330, doi: 10.1109/IMS19712.2021.9574896.

[25] B. K. Tehrani, R. A. Bahr, W. Su, B. S. Cook, and M. M. Tentzeris, "E-band characterization of 3d-printed dielectrics for fully-printed millimeter-wave wireless system packaging," in *Proc. IEEE MTT-S Int. Microw. Symp. (IMS)*, Jun. 2017, pp. 1756–1759, doi: 10.1109/MWSYM.2017.8058985.

[26] "Low loss dielectric 3d printing," 3dfortify.com. https://3dfortify.com/resources/#documentation (Accessed: Dec. 8, 2021).

[27] "3m to showcase industry-first 3d printed PTFE at Formnext," 3m.com. https://news.3m.com/2019-11-18-3M-to-Showcase-Industry-First-3D-Printed-PTFE-at-Formnext (Accessed: Dec. 8, 2021).

[28] B. Tehrani, R. Bahr, D. Revier, B. Cook, and M. Tentzeris, "The principles of" smart" encapsulation: Using additive printing technology for the realization of intelligent application-specific packages for IoT, 5G, and automotive radar applications," in *Proc. IEEE 68th Electron. Components Technol. Conf. (ECTC)*, May 2018, pp. 111–117, doi: 10.1109/ECTC.2018.00025.

[29] A. D. Papadopoulos, B. K. Tehrani, R. A. Bahr, E. M. Tentzeris, and E. N. Glytsis, "Uncertainty quantification of printed microwave interconnects by use of the sparse polynomial chaos expansion method," *IEEE Microw. Compon. Lett.*, vol. 32, no. 1, pp. 1–4, 2022, doi: 10.1109/LMWC.2021.3115618.

[30] L. Li, A. Kapur, and K. B. Heames, "Characterization of transfer molding effects on rf performance of power amplifier module," in *Proc. IEEE 54th Electron. Compon. Technol. Conf. (ECTC)*, 2004, vol. 2, pp. 1671–1677.

[31] A. Yoshida, S. Wen, W. Lin, J. Kim, and K. Ishibashi, "A study on an ultra thin pop using through mold via technology," in *Proc. IEEE 61st Electron. Compon. Technol. Conf. (ECTC)*, May 2011, pp. 1547–1551.

[32] T. Krems, W. Haydl, H. Massler, and J. Rudiger, "Millimeter-wave performance of chip interconnections using wire bonding and flip chip," in *Proc. IEEE MTT-S Int. Microw. Symp. Dig.*, Jun. 1996, vol. 1, pp. 247–250, doi: 10.1109/MWSYM.1996.508504.

[33] B. K. Tehrani and M. M. Tentzeris, "Fully inkjet-printed ramp interconnects for wireless ka-band MMIC devices and multi-chip module packaging," in *Proc. 48th Eur. Microw. Conf. (EuMC)*, Sep. 2018, pp. 1037–1040, doi: 10.23919/EuMC.2018.8541741.

[34] I. Ndip *et al.*, "Modelling the shape, length and radiation characteristics of bond wire antennas," *IET Microw., Antennas Propag.*, vol. 6, no. 10, pp. 1187–1194, Jul. 2012, doi: 10.1049/iet-map.2012.0147.

[35] B. K. Tehrani, B. S. Cook, and M. M. Tentzeris, "Inkjet-printed 3d interconnects for millimeter-wave system-on-package solutions," in *Proc. IEEE MTT-S Int. Microw. Symp. (IMS)*, 2016, pp. 1–4, doi: 10.1109/MWSYM.2016.7540084.

[36] R. Bahr, B. Tehrani, and M. M. Tentzeris, "Exploring 3-d printing for new applications: Novel inkjet- and 3-d-printed millimeter-wave components, interconnects, and systems," *IEEE Microw. Mag.*, vol. 19, no. 1, pp. 57–66, 2018, doi: 10.1109/MMM.2017.2759541.

[37] M. T. Craton, X. Konstantinou, J. D. Albrecht, P. Chahal, and J. Papapolymerou, "A chip-first microwave package using multimaterial aerosol jet printing," *IEEE Trans. Microw. Theory Techn.*, vol. 68, no. 8, pp. 3418–3427, 2020, doi: 10.1109/TMTT.2020.2992074.

[38] A. Eid *et al.*, "Nanotechnology-empowered flexible printed wireless electronics: A review of various applications of printed materials," *IEEE Nanotechnol. Mag.*, vol. 13, no. 1, pp. 18–29, 2019, doi: 10.1109/MNANO.2018.2869233.

Authorized licensed use limited to: Georgia Institute of Technology. Downloaded on August 17,2022 at 17:26:24 UTC from IEEE Xplore. Restrictions apply.